

Multi-decadal modulation of the El Niño–Indian monsoon relationship by Indian Ocean variability

Caroline C Ummerhofer, Alexander Sen Gupta, Yue Li,
Andréa S Taschetto and Matthew H England

Climate Change Research Centre, University of New South Wales, Sydney, Australia

E-mail: c.ummerhofer@unsw.edu.au

Received 13 March 2011

Accepted for publication 20 June 2011

Published 5 July 2011

Online at stacks.iop.org/ERL/6/034006

Abstract

The role of leading modes of Indo-Pacific climate variability is investigated for modulation of the strength of the Indian summer monsoon during the period 1877–2006. In particular, the effect of Indian Ocean conditions on the relationship between the El Niño–Southern Oscillation (ENSO) and the Indian monsoon is explored. Using an extended classification for ENSO and Indian Ocean dipole (IOD) events for the past 130 years and reanalyses, we have expanded previous interannual work to show that variations in Indian Ocean conditions modulate the ENSO–Indian monsoon relationship also on decadal timescales. El Niño events are frequently accompanied by a significantly reduced Indian monsoon and widespread drought conditions due to anomalous subsidence associated with a shift in the descending branch of the zonal Walker circulation. However, for El Niño events that co-occur with positive IOD (pIOD) events, Indian Ocean conditions act to counter El Niño’s drought-inducing subsidence by enhancing moisture convergence over the Indian subcontinent, with an average monsoon season resulting. Decadal modulations of the frequency of independent and combined El Niño and pIOD events are consistent with a strengthened El Niño–Indian monsoon relationship observed at the start of the 20th century and the apparent recent weakening of the El Niño–Indian monsoon relationship.

Keywords: climate variability, Indian monsoon, drought, decadal variability, El Niño–Southern Oscillation, Indian Ocean dipole

1. Introduction

Indian monsoon variability is intricately linked to Pacific Ocean conditions, in particular the El Niño–Southern Oscillation (ENSO). In fact, failure of the Indian monsoon and ensuing droughts and famines at the turn of the 20th century led to the discovery of ENSO by Sir Gilbert Walker. When looking for atmospheric precursors to predict the strength of the Indian monsoon in the 1920s, he identified and recognized the importance of the Southern Oscillation [1, and references therein]. Indian monsoon rainfall is negatively correlated with sea surface temperatures (SST) in the central and eastern equatorial Pacific, with El Niño events generally accompanying a weakening of the Indian summer monsoon

(i.e., June–September; JJAS). The teleconnection from the tropical Pacific to India is due to anomalous subsidence, associated with changes in the zonal Walker circulation, occurring over the Indian subcontinent during El Niño events [2, and references therein].

However, the relationship between El Niño events and the strength of the Indian monsoon is far from perfect, nor is it stationary in time. While generally accounting for 30% of interannual Indian monsoon rainfall variability, ENSO’s impact on the Indian monsoon varies on decadal timescales [1]. Furthermore, [3] reports a weakening of the relationship between the Indian monsoon and ENSO over recent decades. The authors link this to a southeastward shift of the subsiding branch of the anomalous Walker circulation

during recent El Niño events, which allows for normal monsoon development. It has been suggested that the change in the ENSO teleconnection to the Indian monsoon is due to enhanced warming of the Eurasian continent and an amplified land–sea temperature gradient that favours a strengthened Indian monsoon [3]. Alternatively, recent changes in the characteristics of El Niño events have been used to explain the complex ENSO–Indian monsoon relationship. In [2] the authors found that the location of maximum warming along the equatorial Pacific during El Niño events seems to be key for understanding whether drought-producing subsidence occurs over the Indian subcontinent with subsequent monsoon failure: enhanced SST in the central tropical Pacific, rather than the eastern Pacific, more effectively reduces Indian monsoon rainfall. Such modulation of ENSO teleconnections is particularly noteworthy, as the location of maximum El Niño warming has been occurring more frequently in the central Pacific in recent decades [4].

Apart from remote forcing from the Pacific Ocean, SST from the adjacent Indian Ocean also exerts a considerable influence on Indian monsoon variability [5, for example, and references therein]. Pacific and Indian Ocean variability is intricately linked, as manifest in the frequent co-occurrence of ENSO events with the Indian Ocean’s tropical mode of climate variability, the Indian Ocean dipole (IOD) [6, 7]. Several studies [8–10] have explored how the Indian Ocean modulates the ENSO–Indian monsoon teleconnection.

Using the atmospheric general circulation model (AGCM) experiments forced with composite SST anomalies during independent and co-occurring El Niño and positive IOD (pIOD) events, [9] demonstrated that a coincident pIOD event counteracted the monsoon reduction expected from the El Niño-related anomalous subsidence over the Indian subcontinent due to anomalous convergent flow enhancing monsoonal rainfall over the region. Similarly, [10] described negative zonal wind anomalies in the equatorial Indian Ocean related to pIOD events to be associated with above-average monsoon rainfall, despite simultaneous El Niño events occurring. Focusing on conditions early in the Indian monsoon season, [11] found that in some combined pIOD and El Niño years drought may still occur during July (although the rest of the monsoon season returned to more normal rainfall levels). The authors suggested that the occurrence of such a July drought depends upon the timing of the onset of the pIOD, which acts to offset an El Niño-related deficiency in monsoon rainfall during subsequent months. In contrast, analysis by [12] using an index, which combines both ENSO and atmospheric variability in the Indian Ocean basin, found a reinforcing effect of Indian and Pacific Ocean variability on the strength of the Indian summer monsoon for the period 1958–2003.

Recent changes in the Asian monsoon have been reported [13, for example, and references therein] and climate model projections demonstrate the sensitivity of the monsoon to a warming climate. Observed trends in the Indian monsoon have been linked to atmospheric circulation changes associated with low-level divergence and the Somali Jet [13], observed changes in land-use and agricultural intensification [14], and aerosols inducing changes in radiative forcing and in the local Hadley

circulation [15, and references therein], amongst others. Here, we look at how Indo-Pacific conditions have impacted the Indian monsoon over the last 130 years. Over recent decades, non-uniform warming of Indian Ocean temperatures has been reported [16, for example, and references therein], with the eastern Indian Ocean warming less than the west. Consistent with this pIOD-like trend, increasing frequencies of pIOD events have been found in 20th century observations [17]. Given these Indian Ocean trends, the question arises whether a recent weakening of the ENSO–Indian monsoon relationship is in fact driven by changes in ENSO characteristics [2] or in the land–sea temperature contrast [3], or whether increased co-occurrence of pIOD events with El Niño events might be sufficient to explain the weakening relationship. The latter hypothesis is explored here and offers a novel explanation for long-term variations in the ENSO–Indian monsoon teleconnection over the last 130 years due to decadal Indo-Pacific variability.

Drought can have major societal effects over the Indian subcontinent. However, it is subsurface water deficits, more than rainfall itself, that exert stress on agriculture and natural ecosystems. This highlights the importance of focusing on (sub)surface water availability to assess societal impacts associated with drought [18]. The Palmer drought severity index (PDSI), used here as an indicator of drought severity, combines information from both rainfall and surface temperature variability and thus provides an integrative measure of water availability within the ground, being highly correlated with subsurface soil moisture and streamflow conditions [19]. In a review of drought indices, the PDSI has been described to be only of limited use as a short-term monitoring tool for assessing moisture changes on the timescale of several weeks, with questions remaining about its utility in extremely seasonal climates dominated by monsoon dynamics [20, and references therein]. However, the PDSI is used widely and successfully for reconstructing annually resolved drought conditions associated with the summer monsoon across Southeast Asia [21, for example, and references therein], including India. This suggests that it can offer useful insights into the region’s drought conditions associated with Indo-Pacific climate variability across the timescales investigated here.

We expand here on past work [8, 9, in particular] to assess Indian monsoon variability, as well as drought conditions there, during independent and combined pIOD and El Niño events, using a recent classification for ENSO and IOD events over the last 130 years [22, 23]. In particular, decadal modulation of the ENSO–Indian monsoon relationship by Indian Ocean conditions is explored. Thus, our focus on the multi-decadal timescale bridges previous work on interannual variability [8, 9, 12, 10] and recent trends [2, 3]. We also examine how the Indian monsoon variation is linked to large-scale climate anomalies across the Indo-Pacific region.

2. Observations and reanalysis products

For observed Indian precipitation, we use monthly data from the Indian regional/subdivisional monthly rainfall data set by the Indian Institute of Tropical Meteorology [24]. The analyses

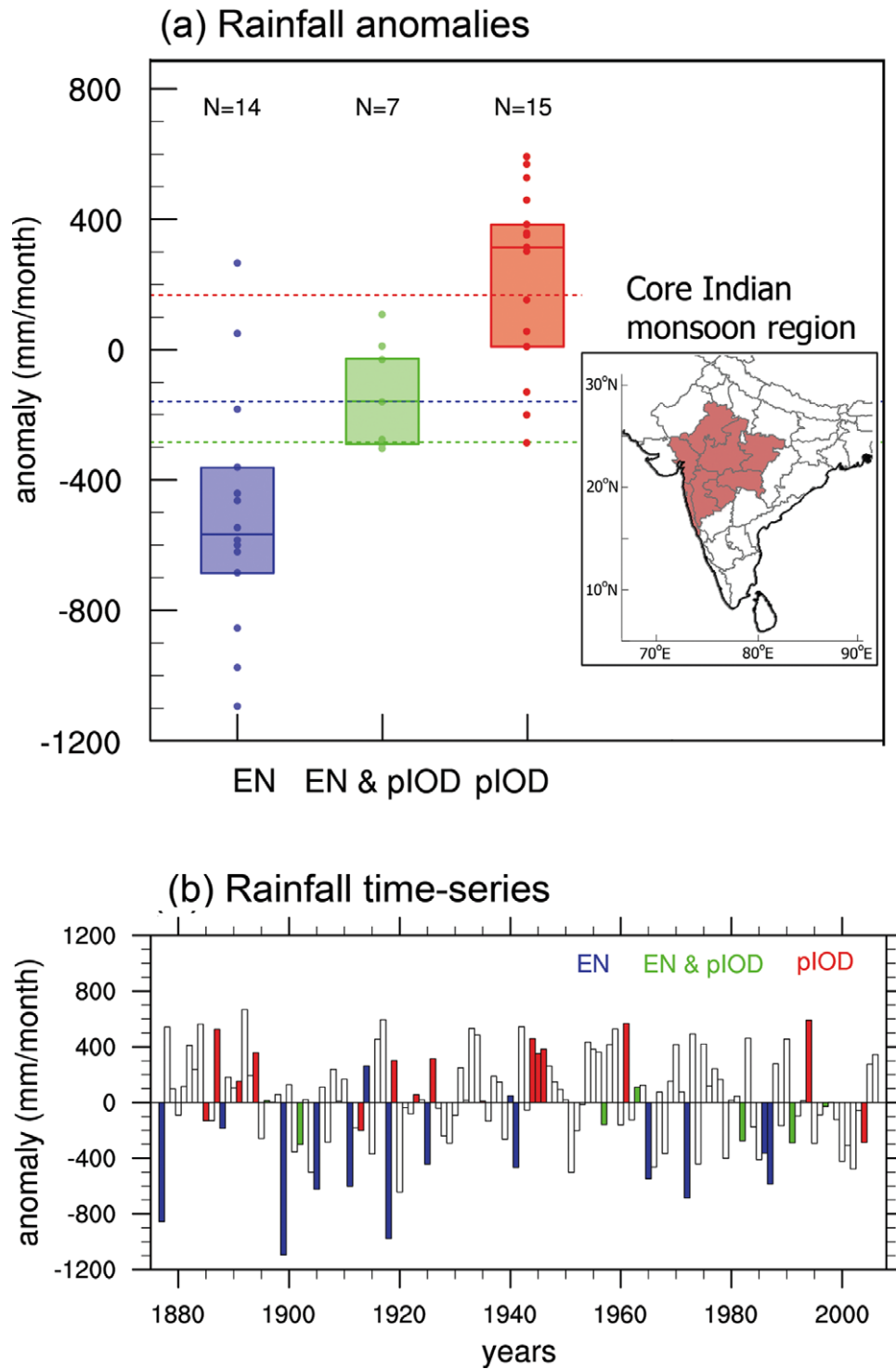


Figure 1. Rainfall anomalies (mm month^{-1}) for the different ENSO/IOD categories for the core Indian monsoon region (see map inset; definition according to IITM; <http://www.tropmet.res.in/IITM/region-maps.html>) during the June–September months for the period 1877–2006: (a) rainfall anomalies shown as dots for El Niño (blue), co-occurring El Niño and pIOD (green), and pIOD (red) events. The colored boxes are delimited by the upper and lower quartiles, with the middle bar denoting the median rainfall in the respective category. Dashed lines indicate the 90% confidence level (as estimated by Monte Carlo testing) for the medians for the different categories (indicated in color), with only the lower threshold shown for the El Niño and co-occurring El Niño with pIOD events and the upper threshold for pIOD events. The number of years (N) in each category is indicated at the top. (b) Time-series of rainfall anomalies with the associated ENSO/IOD categories indicated in color.

here focus on the Indian core monsoon region (see highlighted region in figure 1(a)) for the period 1877–2006 during the summer monsoon (JJAS). To explore the relationship between

Indian monsoon variability and the large-scale circulation associated with ENSO and the IOD we use the classification based on [22], which has been more recently updated in [23].

To investigate large-scale conditions during ENSO/IOD events atmospheric circulation anomalies are assessed with the National Center for Environmental Prediction and the National Center for Atmospheric Research reanalysis (NRR) [25]. Monthly data was used for the period 1948–2006, though all analyses were checked for robustness by using the shorter period 1957–2006 with improved data quality. In addition, rainfall composites were also examined with the Climate Prediction Center Merged Analysis of Precipitation (CMAP) data (1979–2006) [26]. For winds, the 20th century NNR product [27] was also used for the period 1877–2006. SST are taken from the HadISST gridded data set for the period 1877–2006 [28], and the drought index is based on the gridded Dai PDSI for the period 1877–2005 [19]. Given the limitations in the PDSI as a short-term monitoring tool [20], future work could also incorporate more responsive drought indices. Here, however, we are mainly interested in variations of the Indian summer monsoon on multi-decadal timescales, for which the PDSI is suitable and has successfully been applied previously [21, and references therein]. All figures present the analysis with the longest record available to maximize the number of events in the respective categories.

3. Monsoon variability in relation to El Niño and pIOD events

For the Indian core monsoon region (inset figure 1(a)), rainfall anomalies during the summer monsoon (JJAS) for the period 1877–2006 are investigated. To assess the influence of the dominant Indo-Pacific modes of climate variability, anomalous rainfall during El Niño, pIOD, and co-occurring El Niño with pIOD events is presented (figure 1(a)). During El Niño events, median rainfall was significantly reduced by close to 600 mm month⁻¹. Only two El Niño events recorded weakly positive rainfall anomalies, while in excess of 85% of El Niño events showed anomalous dry conditions. More than 20% of El Niño events recorded rainfall deficits in excess of 800 mm month⁻¹. In contrast, El Niño events that co-occurred with a pIOD generally experienced normal rainfall conditions during the summer monsoon. Significantly enhanced rainfall with a median of 300 mm month⁻¹ was recorded for ‘pure’ pIOD events.

A time-series of summer monsoon rainfall between 1877 and 2006, with the different ENSO/IOD events highlighted, confirms these results (figure 1(b)): the majority of ‘pure’ El Niño events coincided with large deficits in Indian monsoonal rainfall, while ‘pure’ pIOD events were generally associated with anomalous wet conditions. Co-occurring El Niño and pIOD years showed normal levels of rainfall. Severe monsoon failures during El Niño events occurred between 1899 and 1925 (figure 1(b)). In contrast, the period 1926–64 only experienced two El Niño events, one of which was associated with a large deficit in monsoonal rainfall, while a similarly dry year (1920) occurred independent of ENSO or IOD events. During this same period, several consecutive pIOD events coincided with anomalous wet conditions for the Indian core monsoon region. These results highlight the presence

Table 1. Number of independent and combined El Niño and pIOD events and mean JJAS Indian monsoon rainfall (in mm), ±1 standard deviation (SD) during four separate multi-decadal periods of the observational record. Bold type numbers indicate values that are significant at the 90% confidence level for the number of events and at the 75% confidence level for rainfall, based on Monte Carlo analyses. Over the period 1877–2006, mean JJAS rainfall was 2200 mm, with an SD of 356 mm.

	Number of events			Rainfall (±1 SD)
	EN and pIOD	EN	pIOD	
1877–1910	2	4	4	2202 (±387)
1911–42	0	6	5	2173 (±374)
1943–74	2	2	4	2267 (±352)
1975–2006	3	2	2	2155 (±310)

of considerable decadal variability across the tropical Indo-Pacific region [29, for example].

Given the decadal modulation in the tropical Indo-Pacific modes of variability, it is of interest to explore whether this contributes to modulations in the strength of the ENSO–Indian monsoon relationship. Table 1 presents the number of independent and co-occurring El Niño and pIOD events over the last 130 years during four multi-decadal periods, as well as mean JJAS Indian monsoon rainfall and its standard deviation over the four periods. Using a Monte Carlo test, random multi-decadal periods are compared with these four observed periods. This was repeated 25 000 times to determine whether the numbers of El Niño and pIOD events (mean rainfall) recorded in each multi-decadal period were unusual. Despite obtaining some statistically significant results, we would still caution that the analysis relies on relatively few events.

Over the last three decades, there were three incidents of co-occurring pIOD and El Niño events, while only two independent El Niño and pIOD events each occurred (table 1). This indicates a significantly enhanced occurrence of combined events during this period and a significantly reduced incidence in the number of independent events. The latter contributes to the lowest standard deviation (SD; 310 mm) in mean rainfall recorded for any of the four periods (table 1). The period 1943–74 is characterized by a significant reduction in El Niño, but with twice as many pIOD events. This is manifest as a significantly increased mean JJAS rainfall. The two earlier periods do not show significant anomalies in mean rainfall, most likely due to a compensating increase in the frequency of wet pIOD and dry El Niño events, as reflected in the high SD. During the period 1911–42, six independent El Niño events occurred and remarkably no combined event. This is unprecedented during any part of the 130 year record. The period without any single co-occurring El Niño and pIOD event actually extends from 1903 to 1956 (cf figure 1(b)). This is in marked contrast to the latter half of the historical record, when 5 combined events have occurred post-1957. Multi-decadal Indian Ocean variability, as manifest in the frequency of IOD events, could potentially play an important role in controlling the Indian monsoon through modulation of the ENSO–Indian monsoon relationship.

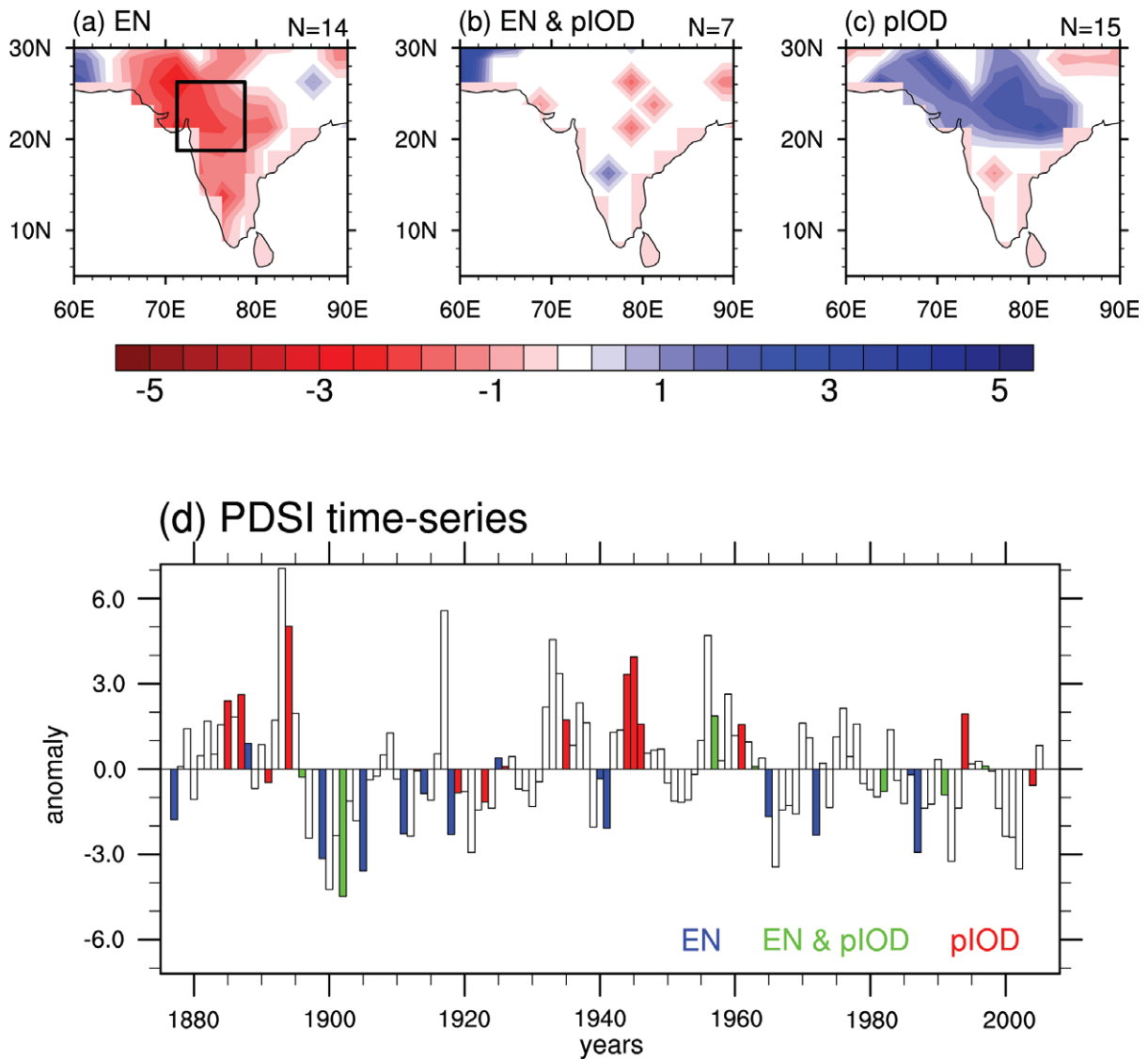


Figure 2. Composite PDSI anomalies during (a) El Niño, (b) combined El Niño and pIOD, and (c) pIOD events averaged for the June–September months for the period 1877–2005. Only anomalies are shown that are significant at the 80% confidence level as estimated by a two-tailed *t*-test. (d) Time-series of PDSI anomalies spatially averaged over the core monsoon region (black box in (a) indicated) with the associated ENSO/IOD categories indicated in color.

4. Drought variability in relation to El Niño and pIOD events

Composites of PDSI for El Niño, pIOD, and co-occurring events highlight the distinct impacts of the two modes on drought across the Indian subcontinent (figures 2(a)–(c)). During El Niño events, much of India suffers drought conditions (figure 2(a)). This is particularly apparent in the centre and northwest regions that make up the core monsoon region (cf inset figure 1(a)): PDSI values are in excess of -3 indicating severe drought conditions. In contrast, no consistent large-scale features in drought incidence are observed during co-occurring El Niño and pIOD events (figure 2(b)). Anomalous wet conditions with a PDSI in excess of $+2$ are found during pIOD events for the northern half of the Indian subcontinent (figure 2(c)).

The PDSI time-series spatially averaged over the Indian core monsoon region (see box in figure 2(a)) for the period 1877–2006 shows that more than 85% of El Niño events were associated with negative PDSI values (figure 2(d)). About 50% of El Niño events were associated with very severe drought conditions, while more than 60% of pIOD events had PDSI values in excess of $+1$. Decadal variability in the PDSI time-series related to changes in the numbers of ENSO and IOD events matches that seen from the rainfall time-series (cf table 1 and figure 1).

5. Climate conditions during El Niño and pIOD events

For a better understanding of the contrasting rainfall and drought responses associated with the different mode phases,

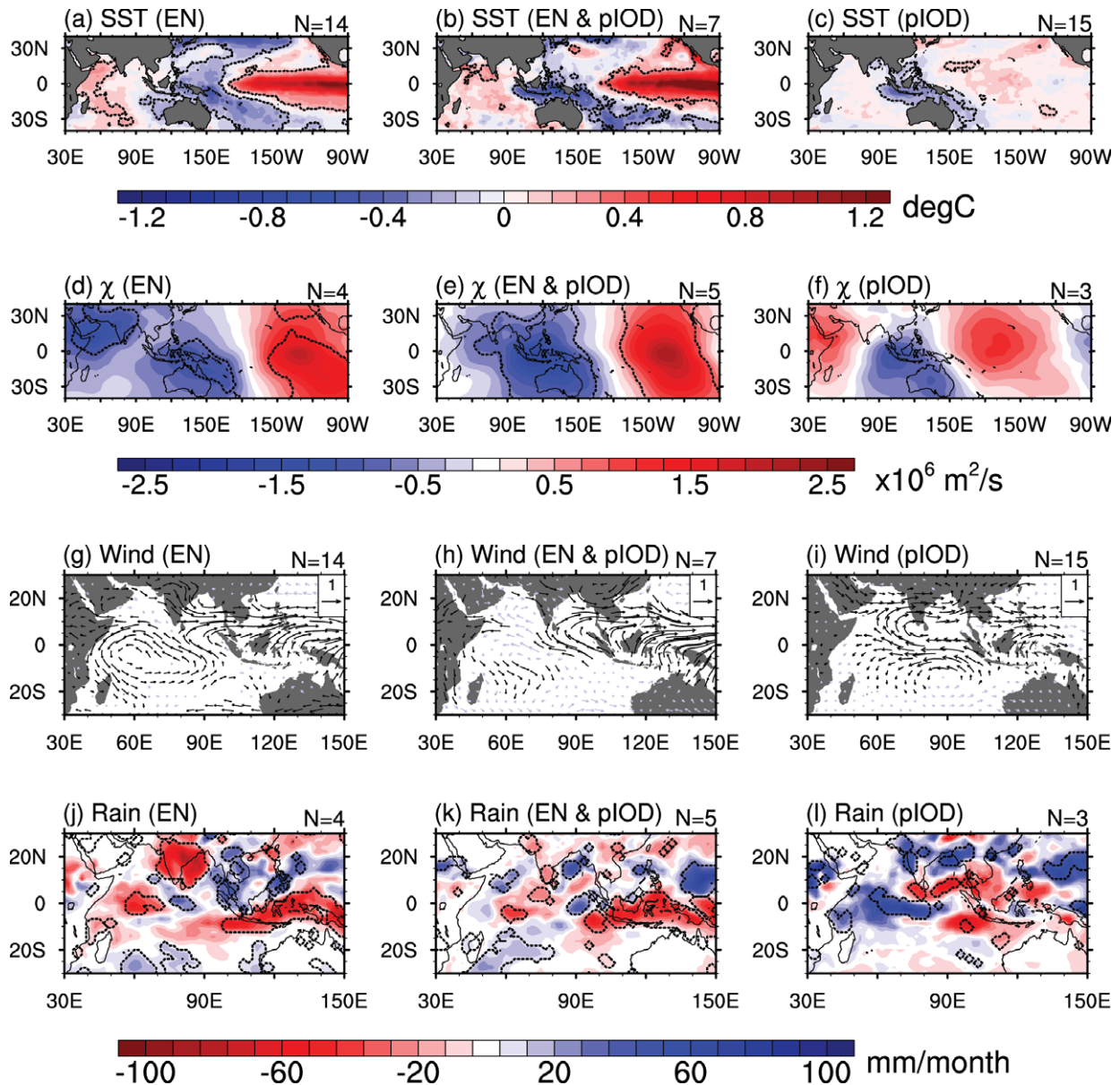


Figure 3. Composite anomalies during (left) El Niño, (middle) combined El Niño and pIOD, and (right) pIOD events averaged for the June–September months for (a)–(c) SST ($^{\circ}\text{C}$), (d)–(f) 850 hPa velocity potential χ ($\text{m}^2 \text{s}^{-1}$), (g)–(i) 850 hPa winds (m s^{-1}), and (j)–(l) rainfall (mm month^{-1}). Anomalies for χ and rainfall are based on the period 1948–2006, SST and winds on 1877–2006. The number of members (N) in each category is indicated. The area enclosed by the dashed contours and the black arrows denote anomalies that are significant as estimated by a two-tailed t -test at the following confidence levels: 90% for SST and χ , and 80% for winds and rainfall.

the anomalous large-scale circulation features across the Indo-Pacific region are explored for El Niño, pIOD, and the co-occurrence of these events (figure 3). For the three respective event categories, composite anomalies are shown for SST, velocity potential χ , winds, and rainfall. A higher number of events in the composites exist for SST and winds, as the analysis is over the 1877–2006 period, while the shorter period 1948–2006 is used for the other variables due to the constraints in data availability (cf section 2). The larger spatial extent of significant anomalies in figures 3(a)–(c) and (g)–(i) can largely be attributed to this fact. The winds are presented at the 850 hPa level, which is well suited to the study of monsoon dynamics [30]. Velocity potential, which

provides an indication of subsidence associated with the large-scale circulation, is shown at the same level for consistency. Anomalies in the velocity potential at 200 hPa (figure not shown) highlight a comparable pattern, but of opposite sign, confirming the low-level results.

Pure El Niño events are characterized by warm SST anomalies, exceeding 1.5°C , in the eastern equatorial Pacific, surrounded by cold anomalies in the classical ‘horseshoe’ pattern in the subtropics and western tropical Pacific (figure 3(a)). In the Indian Ocean, warm (cold) SST anomalies are observed in the western (eastern) tropical region. The cold SST anomalies in the eastern Indian Ocean are mainly located off the northwest shelf of Australia, south of the

IOD eastern pole of [6]. The velocity potential shows anomalous rising motion over the eastern Pacific, while anomalous subsidence occurs over the western Pacific warm pool region, the Maritime Continent, and the Australian region (figure 3(d)). In addition, an anticyclonic anomaly associated with anomalous subsidence is also observed over the Indian subcontinent extending west across the Indian Ocean towards East Africa. The regional winds at 850 hPa are consistent with the anomalous subsidence over India, with easterly anomalies over the Arabian Sea (5°–20°N) extending from India to the East African coastline (figure 3(g)). The easterly wind anomalies represent a weakening of the moisture-bearing onshore westerlies during the Indian summer monsoon, and this is consistent with the anomalous dry conditions during El Niño years (figure 3(j)).

For pIOD events, the cold SST anomalies around the Maritime Continent dominate (figure 3(b)) due to enhanced upwelling and southeasterly anomalies in the equatorial eastern Indian Ocean (figure 3(i)). There is a suggestion of moderate anomalous subsidence over the Australian region, flanked by two regions of anomalous ascent over eastern Africa and the central Pacific (figure 3(f)), however, the values are not statistically significant. Significantly enhanced westerly winds are, however, observed over the northern Indian Ocean, including the Arabian Sea, Bay of Bengal, and India (figure 3(i)), accounting for anomalous wet conditions across western India and the core monsoon region during pIOD events (figure 3(l)).

During co-occurring El Niño and pIOD years, the warm equatorial SST anomalies in the eastern Pacific are enhanced relative to pure El Niño events (cf figures 3(a) and (b)). The cold anomalies are clearly apparent in the eastern tropical Indian Ocean, around the Maritime Continent, and western Pacific warm pool region (figure 3(b)), while only a localized area of above-average SST can be seen to the west of the Indian subcontinent. Consistent with the SST anomaly pattern, anomalous ascending motion is observed over the eastern Pacific. Anomalous subsidence dominates across the western Pacific and eastern Indian Ocean, with the centre of subsidence located over the Maritime Continent and India at the western edge of the anomalous vertical motion (figure 3(e)). Consequently over India, the winds at 850 hPa do not show any significant changes during co-occurring El Niño and pIOD events (figure 3(h)), nor are there any significant rainfall anomalies except in a few very localized regions (figure 3(k)).

6. Discussion and conclusions

We have assessed the impact of El Niño and pIOD events, both individually and in combination, on the Indian summer monsoon season (JJAS) for the period 1877–2006. The majority of pure El Niño events are associated with significant reductions in monsoon rainfall and widespread drought conditions due to anomalous subsidence over the Indian subcontinent, associated with changes in the zonal Walker circulation and weakening of the onshore monsoon circulation over India. This is consistent with previous work detailing

the mechanisms for Indian monsoon failure during El Niño events [3, 9, 2, for example]. In contrast, during pure pIOD events increased rainfall generally occurs due to an intensified monsoon circulation, resulting in anomalously enhanced positive PDSI values. During co-occurring pIOD and El Niño events, the El Niño-modulation of Indian monsoon rainfall is absent and normal rainfall levels are maintained. During combined events there is anomalous subsidence associated with the Indo-Pacific SST anomaly pattern centered over the Maritime Continent, as also shown by [9] in AGCM simulations.

Using a classification for ENSO and IOD events for the past 130 years, we have expanded on previous observational studies [8, for example] and shown that decadal variations in Indian Ocean conditions modulate the ENSO–Indian monsoon relationship. In the first half of the 20th century, six El Niño events were accompanied by severe Indian monsoon failures; this period is notable for a prolonged absence of co-occurring pIOD and El Niño events and high JJAS monsoon rainfall variability. In contrast, a trend towards more frequent pIOD events has occurred over recent decades [17]; this is reflected in a significantly enhanced incidence of co-occurring pIOD and El Niño events post-1975, the lowest interannual monsoon variability observed over the last 130 years, and a reduced frequency of pure El Niño events. Recent trends in tropical Indian Ocean variability are therefore able to help explain the weakening relationship between ENSO and the Indian monsoon, adding to previous explanations of changing land–sea temperature gradients [3] and the characteristics of El Niño events [2]. The role of the Pacific Ocean in forcing recent Indian Ocean trends, as well as modulating decadal variability within that basin, remains to be assessed.

In summary, whether an El Niño event causes a failure of the Indian monsoon and resulting drought conditions can largely be determined by the state of the Indian Ocean. Earlier work has demonstrated that the modulation of the monsoon by El Niño depends on the location of maximum warming in the equatorial Pacific [2]. Here, we demonstrate that changes in Indian Ocean variability play an important role in modulating the ENSO-related monsoon rainfall response on multi-decadal timescales.

Acknowledgments

We are grateful for the following data sets: Indian regional/subdivisional Monthly Rainfall by the Indian Institute of Tropical Meteorology; HadISST by the UK Met Office; PDSI, CMAP, and NNR provided by NOAA/OAR/ESRL PSD, Boulder, Colorado, USA. Two anonymous reviewers are gratefully acknowledged for their helpful comments. This work was supported by the Australian Research Council.

References

- [1] Webster P J and Hoyos C D 2010 Beyond the spring barrier? *Nat. Geosci.* **3** 152–3
- [2] Krishna Kumar K, Rajagopalan B, Hoerling M P, Bates G and Cane M 2006 Unraveling the mystery of Indian monsoon failure during El Niño *Science* **314** 115–9

- [3] Krishna Kumar K, Rajagopalan B and Cane M A 1999 On the weakening relationship between the Indian monsoon and ENSO *Science* **284** 2156–9
- [4] Ashok K, Behera S K, Rao S A, Weng H and Yamagata T 2007 El Niño Modoki and its possible teleconnection *J. Geophys. Res.* **112** C11007
- [5] Schott F A, Xie S-P and McCreary J P 2009 Indian Ocean variability and climate variability *Rev. Geophys.* **47** RG1002
- [6] Saji N H, Goswami B N, Vinayachandran P N and Yamagata T 1999 A dipole mode in the tropical Indian Ocean *Nature* **401** 360–3
- [7] Webster P J, Moore A M, Loschnigg J P and Leben R R 1999 Coupled ocean–atmosphere dynamics in the Indian Ocean during 1997–98 *Nature* **401** 356–60
- [8] Ashok K, Guan Z and Yamagata T 2001 Impact of the Indian Ocean dipole on the relationship between the Indian monsoon rainfall and ENSO *Geophys. Res. Lett.* **28** 4499–502
- [9] Ashok K, Guan Z, Saji N H and Yamagata T 2004 Individual and combined influences of the ENSO and Indian Ocean dipole on the Indian summer monsoon *J. Clim.* **17** 3141–55
- [10] Ihara C, Kushnir Y, Cane M A and De la Pena V H 2007 Indian summer monsoon rainfall and its link with ENSO and Indian Ocean climate indices *Int. J. Climatol.* **27** 179–87
- [11] Ihara C, Kushnir Y and Cane M A 2008 July droughts over homogeneous Indian Monsoon region and Indian Ocean dipole during El Niño events *Int. J. Climatol.* **28** 1799–805
- [12] Gadgil S, Vinayachandran P N, Francis P A and Gadgil S 2004 Extremes of the Indian summer monsoon rainfall, ENSO and equatorial Indian Ocean oscillation *Geophys. Res. Lett.* **31** L12213
- [13] Turner A G and Hannachi A 2010 Is there regime behaviour in monsoon convection in the late 20th century? *Geophys. Res. Lett.* **37** L16706
- [14] Niyogi D, Kishtawal C, Tripathi S and Govindaraju R S 2010 Observational evidence that agricultural intensification and land use change may be reducing the Indian summer monsoon rainfall *Water Resour. Res.* **46** W03533
- [15] Ji Z, Kang S, Zhang D, Zhu C, Wu J and Xu Y 2011 Simulation of the anthropogenic aerosols over South Asia and their effects on Indian summer monsoon *Clim. Dyn.* **36** 1633–47
- [16] Ihara C, Kushnir Y and Cane M A 2008 Warming trend of the Indian Ocean SST Indian Ocean dipole from 1880 to 2004 *J. Clim.* **21** 2035–46
- [17] Cai W, Cowan T and Sullivan A 2009 Recent unprecedented skewness towards positive Indian Ocean dipole occurrences and their impact on Australian rainfall *Geophys. Res. Lett.* **36** L11705
- [18] LeBlanc M J, Tregoning P, Ramillien G, Tweed S O and Fakes A 2009 Basin-scale, integrated observations of the early 21st century multiyear drought in southeast Australia *Water Resour. Res.* **45** W04408
- [19] Dai A, Trenberth K E and Qian T 2004 A global data set of Palmer drought severity index for 1870–2002: relationship with soil moisture and effects of surface warming *J. Hydrometeorol.* **5** 1117–30
- [20] Smakhtin V U and Hughes D A 2004 Review, automated estimation and analyses of drought indices in South Asia *Working Paper 83* (Colombo, Sri Lanka: International Water Management Institute) p 24
- [21] Cook E R, Anchukaitis K J, Buckley B M, D’Arrigo R D, Jacoby G C and Wright W E 2010 Asian monsoon failure and megadrought during the last millennium *Science* **328** 486–9
- [22] Meyers G, McIntosh P, Pigot L and Pook M 2007 The years of El Niño, La Niña and interactions with the tropical Indian Ocean *J. Clim.* **20** 2872–80
- [23] Ummenhofer C C, England M H, Meyers G A, McIntosh P C, Pook M J, Risbey J S, Sen Gupta A and Taschetto A S 2009 What causes Southeast Australia’s worst droughts? *Geophys. Res. Lett.* **36** L04706
- [24] Parthasarathy B, Munot A A and Kothawale D R 1994 All India monthly and seasonal rainfall series: 1871–1993 *Theor. Appl. Climatol.* **49** 217–24
- [25] Kistler R *et al* 2001 The NCEP-NCAR 50-year reanalysis: monthly means CD-ROM and documentation *Bull. Am. Meteorol. Soc.* **82** 247–67
- [26] Xie P and Arkin P A 1996 Analyses of global monthly precipitation using gauge observations, satellite estimates, and numerical model predictions *J. Clim.* **9** 840–58
- [27] Compo G P, Whitaker J S and Sardeshmukh P D 2006 Feasibility of a 100 year reanalysis using only surface pressure data *Bull. Am. Meteorol. Soc.* **87** 175–90
- [28] Rayner N A, Parker D E, Horton E B, Folland C K, Alexander L V and Rowell D P 2003 Global analyses of SST, sea ice and night marine air temperature since the late nineteenth century *J. Geophys. Res.* **108** 4407–35
- [29] D’Arrigo R, Abram N, Ummenhofer C, Palmer J and Mudelsee M 2011 Reconstructed streamflow for Citarum River, Java, Indonesia: linkages to tropical climate dynamics *Clim. Dyn.* **36** 451–62
- [30] Webster P J, Magana V O, Palmer T N, Shukla J, Tomas R A, Yanai M and Yasunari T 1998 Monsoons: processes, predictability, and the prospects for prediction *J. Geophys. Res.* **103** 14451–510